Enhancing resonances of optical nanoantennas by circular gratings

Jing Qi,[1] **Thomas Kaiser,**[2] **Angela E. Klein,**[2] **Michael Steinert,**[2] **Thomas Pertsch,**[2] **Falk Lederer,**[1] **and Carsten Rockstuhl**[1,3,4,*]

[1] *Institute of Condensed Matter Theory and Solid State Optics, Abbe Center of Photonics, Friedrich-Schiller-Universität Jena, Max-Wien-Platz 1, 07743 Jena, Germany*
[2] *Institute of Applied Physics, Abbe Center of Photonics, Friedrich-Schiller-Universität Jena, Max-Wien-Platz 1, 07743 Jena, Germany*
[3] *Institute of Theoretical Solid State Physics, Karlsruhe Institute of Technology, Wolfgang-Gaede-Strasse 1, 76131 Karlsruhe, Germany*
[4] *Institute of Nanotechnology, Karlsruhe Institute of Technology, P.O. Box 3640, 76021 Karlsruhe, Germany*

[*] *carsten.rockstuhl@kit.edu*

Abstract: Optical plasmonic antennas allow for localizing and enhancing light at the nanoscale. To enhance the application opportunities of optical antennas, their quality factor needs to be substantially improved. Here, we numerically and experimentally demonstrate that the resonance of a dipolar metallic disc antenna can be enhanced by a circular grating that obeys the Bragg condition. The supporting grating effectively collects energy from an extended spatial domain and guides it spectrally-selected into the central antenna, leading to a significantly enhanced field intensity at resonance. Accordingly, the quality factor of the antenna is enhanced by at least five times. The approach can be applied to other plasmonic systems, hence constituting an important ingredient to a future plasmonic tool box.

OCIS codes: (230.1480) Bragg reflectors; (250.5403) Plasmonics; (230.5750) Resonators; (260.3910) Metal optics; (310.6628) Subwavelength structures, nanostructures.

References and links

1. L. Novotny and N. van Hulst, "Antennas for light," Nature Photon. **5,** 83–90 (2011).
2. P. Bharadwaj, B. Deutsch, and L. Novotny, "Optical antennas," Adv. Opt. Photon. **1**(3), 438–483 (2009).
3. J. Dorfmüller, R. Vogelgesang, W. Khunsin, C. Rockstuhl, C. Etrich, and K. Kern, "Plasmonic nanowire antennas: experiment, simulation, and theory," Nano Lett. **10**(9), 3596–3603 (2010).
4. T. H. Taminiau, F. D. Stefani, and N. F. van Hulst, "Optical Nanorod Antennas Modeled as Cavities for Dipolar Emitters: Evolution of Sub- and Super-Radiant Modes," Nano Lett. **11**(3), 1020–1024 (2011).
5. B. A. Saleh and M. C. Teich, *Fundamentals of Photonics* (Wiley, 1991), pp. 310–341.
6. G. V. Naik, V. M. Shalaev, and A. Boltasseva, "Alternative Plasmonic Materials: Beyond Gold and Silver," Adv. Mater. **25**(24), 3264–3294 (2013).
7. M. Kuttge, F. J. García de Abajo, and A. Polman, "Ultrasmall Mode Volume Plasmonic Nanodisk Resonators," Nano Lett. **10**(5), 1537–1541 (2011).
8. R. Filter, J. Qi, C. Rockstuhl, and F. Lederer, "Circular optical nanoantennas: an analytical theory," Phys. Rev. B **85**(12), 125429 (2012).
9. N. Liu, M. Mesch, T. Weiss, M. Hentschel, and H. Giessen, "Infrared Perfect Absorber and Its Application As Plasmonic Sensor," Nano Lett. **10**(7), 2342–2348 (2010).
10. C. Rockstuhl and F. Lederer, "Photon management by metallic nanodiscs in thin film solar cells," Appl. Phys. Lett. **94**(21), 213102 (2009).
11. R. Esteban, T. V. Teperik, and J. J. Greffet, "Optical Patch Antennas for Single Photon Emission Using Surface Plasmon Resonances," Phys. Rev. Lett. **104**(2), 026802 (2010).

#236122 - $15.00 USD Received 12 Mar 2015; revised 16 May 2015; accepted 18 May 2015; published 26 May 2015

12. Z. Liu, J. M. Steele, W. Srituravanich, Y. Pikus, C. Sun, and X. Zhang, "Focusing Surface Plasmons with a Plamonic Lens," Nano Lett. **5**(9), 1726–1729 (2005).
13. W. Chen, D. C. Abeysinghe, R. L. Nelson, and Q. Zhan, "Plasmonic Lens Made of Multiple Concentric Metallic Rings under Radially Polarized Illumination," Nano Lett. **9**(12), 4320–4325 (2009).
14. G. M. Lerman, A. Yanai, and U. Levy, "Demonstration of Nanofocusing by the use of Plasmonic Lens Illuminated with Radially Polarized Light," Nano Lett. **9**(5), 2139–2143 (2009).
15. G. Lévêque and O. J. F Martin, "Optimization of finite diffraction gratings for the excitation of surface plasmon," J. Appl. Phys. **100**(12), 124301 (2006).
16. A. Baron, E. Devaux, J-C. Rodier, J. P. Hugonin, E. Rousseau, C. Genet, T. W. Ebbesen, and P. Lalanne, "Compact Antenna for Efficient and Unidirectional Launching and Decoupling of Surface Plasmons," Nano Lett. **11**(10), 4207–4212 (2011).
17. C. Chen and P. Berini, "Grating couplers for broadside input and output coupling of long-range surface plasmons," Opt. Express **18**(8), 8006–8018 (2010).
18. G. Li, L. Cai, F. Xiao, Y. Pei, and A. Xu, "A quantitative theory and the generalized Bragg condition for surface plasmon Bragg reflectors," Opt. Express **18**(10), 10487–10499 (2010).
19. W. Cai, A. P. Vasudev, and M. L. Brongersma, "Electrically Controlled Nonlinear Generation of Light with Plasmonics," Science **333**, 1720–1723 (2011).
20. F. López-Tejeira, S. G. Rodrigo, L. Martín-Moreno, F. J. García-Vidal, E. Devaux, T. W. Ebbesen, J. R. Krenn, I. P. Radko, S. I. Bozhevolnyi, M. U. González, J. C. Weeber, and A. Dereux, "Efficient unidirectional nanoslit couplers for surface plasmons," Nature Phys. **3**, 324–328 (2007).
21. A. Hosseini, H. Nejati, and Y. Massoud, "Modeling and design methodology for metal-insulator-metal plasmonic Bragg reflectors," Opt. Express **16**(3), 1475–1480 (2008).
22. H. J. Lezec, A. Degiron, E. Devaux, R. A. Linke, L. Martín-Moreno, F. J. García-Vidal, and T. W. Ebbesen, "Beaming Light from a Subwavelength Aperture," Science **297**, 820–822 (2002).
23. S. Carretero-Palacios, O. Mahboub, F. J. Garcia-Vidal, L. Martin-Moreno, Sergio G. Rodrigo, C. Genet, and T. W. Ebbesen, "Mechanisms for extraordinary optical transmission through bulls eye structures," Opt. Express **19**(11), 10429–10442 (2011).
24. A. Degiron and T. W. Ebbesen, "Analysis of the transmission process through single apertures surrounded by periodic corrugations," Opt. Express **12**(16), 3694–3700 (2004).
25. O. Mahboub, S. Carretero Palacios, C. Genet, F. J. García-Vida, S. G. Rodrigo, L. Martín-Moreno, and T. W. Ebbesen, "Optimization of bulls eye structures for transmission enhancement," Opt. Express **18**(11), 11292–11299 (2010).
26. H. Aouani, O. Mahboub, E. Devaux, H. Rigneault, T. W. Ebbesen, and J. Wenger, "Plasmonic Antennas for Directional Sorting of Fluorescence Emission," Nano Lett. **11**(6), 2400–2406 (2011).
27. H. Aouani, O. Mahboub, N. Bonod, E. Devaux, E. Popov, H. Rigneault, T. W. Ebbesen, and J. Wenger, "Bright Unidirectional Fluorescence Emission of Molecules in a Nanoaperture with Plasmonic Corrugations," Nano Lett. **11**(2), 637–644 (2011).
28. J. T. Choy, I. Bulu, B. J. M. Hausmann, E. Janitz, I-C.Huang, and M. Lončar, "Spontaneous emission and collection efficiency enhancement of single emitters in diamond via plasmonic cavities and gratings," Appl. Phys. Lett. **103**(16), 161101 (2013).
29. D. Wang, T. Yang, and K. B. Crozier, "Optical antennas integrated with concentric ring gratings: electric field enhancement and directional radiation," Opt. Express **19**(3), 2148–2157 (2011).
30. S. Maier, *Plasmonics: Fundamentals and Applications* (Springer, 2007), pp. 21–34.
31. B. Prade, J. Y. Vinet, and A. Mysyrowicz, "Guided optical waves in planar heterostructures with negative dielectric constant," Phys. Rev. B **44**(24), 13556 (1991).
32. S. B. Hasan, R. Filter, A. Ahmed, R. Vogelgesang, R. Gordon, C. Rockstuhl, and F. Lederer, "Relating localized nanoparticle resonances to an associated antenna problem," Phys. Rev. B **84**(19), 195405 (2011).
33. A. Hänsel, O. A. Egorov, S. B. Hasan, C. Rockstuhl, and F. Lederer, "Optical bistability in a doubly resonant $\chi^{(2)}$-nonlinear plasmonic nanocavity," Phys. Rev. A **85**(5), 053843 (2012).
34. J. Qi, T. Kaiser, R. Peuker, T. Pertsch, F. Lederer, and C. Rockstuhl, "Highly resonant and directional optical nanoantennas," J. Opt. Soc. Am. A **31**(2), 388–393 (2014).
35. K. S. Yee, "Numerical Solution of Initial Boundary Value Problems Involving Maxwells Equations in Isotropic Media," IEEE Trans. Antennas Propag. **AP14**(3), 302–307 (1966).
36. A. F. Oskooi, D. Roundy, M. Ibanescu, P. Bermel, J. D. Joannopoulos, and S. G. Johnson, "Meep: A flexible free-software package for electromagnetic simulations by the FDTD method," Comput. Phys. Commun. **181**(3), 687–702 (2010).

1. Introduction

Metallic optical antennas have been intensively studied as one of the fundamental constituents of nanophotonics. A simple picture to understand the emergence of their resonances is an ex-

#236122 - $15.00 USD Received 12 Mar 2015; revised 16 May 2015; accepted 18 May 2015; published 26 May 2015

trapolation from ordinary resonators [1–4].

At the scale of nanometers, these subwavelength resonators are formed by truncating a metallic film that supports propagating surface plasmonic polaritons (SPPs). The continuous spectrum of SPP modes is discretized and standing waves emerge from SPPs bouncing back and forth in the finite geometry. At resonance, the phase accumulation of SPPs per round trip equals a multiple of 2π. This includes the phase accumulation upon propagation and a contribution from a complex valued reflection coefficient at the terminations. The lowest order resonance is dipolar that persists also in the quasi-static limit. Then, the 2π phase accumulation per round trip originates mainly from the phase of the reflection coefficient. When an optical antenna is resonantly excited, the field intensity is largely enhanced and strongly localized around the subwavelength resonator. This enables versatile applications.

To characterize a resonance of an optical nanoantenna, the quality factor is usually considered as a crucial criterion [5]. It interprets the number of round trips a SPP experiences prior to its eventual dissipation. The quality factor of a plasmonic antenna is limited by two processes. One process is associated with intrinsic properties of the materials, i.e. absorption in metals. This nonradiative loss is described by the imaginary part of the propagation constant of the SPPs. Although tremendous research efforts are currently devoted to identify more suitable plasmonic materials [6], such dissipation cannot be avoided.

The other limitation of the quality factor is set by radiative losses. This process is described by a reflection coefficient that is smaller than unity. The reflection coefficient, contrary to the dissipative losses, can be tailored by design. Inspired by dielectric Bragg gratings whose reflectivity can be close to unity for an ordinary resonator, we explore the possibility to integrate the same structure into a subwavelength resonator. This potentially reinforces the field in a narrow spectral domain, leading to an enhancement of the antenna's quality factor. For this purpose, we explore a nanodisc antenna endowed by a plasmonic Bragg grating with numerical and experimental means.

The nanodisc has been chosen while considering it as a fundamental subwavelength resonator [7, 8], which enables various applications such as assisting biological and chemical sensing [9], increasing the solar cell efficiency [10], and enabling single photon emission if adjoined with quantum emitters [11]. In this work we are concerned with the nanoantenna working in the receiving mode, i.e. the nanodisc antenna is considered as a subwavelength resonator where only the localized SPPs modes are supported. The purpose of the nanoantenna in the receiving mode is to collect and localize an external light source to the nanoscale, i.e. to receive locally light. Note this is different from the previous study on propagating SPPs in large circular metallic plates [12–14].

Plasmonic gratings as the second ingredient, in general, are well studied in nanophotonics. They are mostly used as plasmonic couplers where they compensate the momentum mismatch between the light in free space and propagating SPPs [15–17] or as plasmonic Bragg mirrors for propagating SPPs at extended interfaces [18–21]. Normally, they are considered as one-dimensional structures that are infinitely extended in the perpendicular direction. In the last decade, radial structures where the line gratings are transformed into a group of concentric rings have been investigated as well. Compared to one-dimensional gratings, such circular gratings provide omnidirectional reflections, preventing the lateral leakage of light from the center. This ensures a two-dimensional field confinement. It has been theoretically and experimentally verified that circular plasmonic gratings can lower the divergence of transmitted light from subwavelength apertures [22, 23] and effectively overcome the diffraction limit [24, 25]. These features suggested further exploitations of circular gratings and the application regime has been largely broadened in the more recent past. For instance, circular gratings have been used to directionally control the fluorescence emission from molecules [26,27] and can increase

#236122 - $15.00 USD Received 12 Mar 2015; revised 16 May 2015; accepted 18 May 2015; published 26 May 2015

the radiation efficiency of the encircled quantum emitters [28]. It also has been reported that circular gratings can intensify the electric field of the enclosed nanoantenna and they have been proposed for the enhancement of Raman scattering [29].

In this paper, we use the nanodisc antenna as an example to illustrate that a few concentric rings are sufficient to construct a fully functional circular grating that can reinforce the resonance of the enclosed resonator. In the following, we first discuss the basic properties for structures embedded in a symmetric optical environment, i.e. in a homogenous isotropic dielectric material. Afterwards, we extend the discussion to the asymmetric optical environment, i.e. the resonator and the supporting grating are deposited on a substrate. This prepares the analysis on the experimental results of field enhancement of different samples in real space measured by a scanning near field optical microscope (SNOM).

2. Circular grating endowed disc resonator

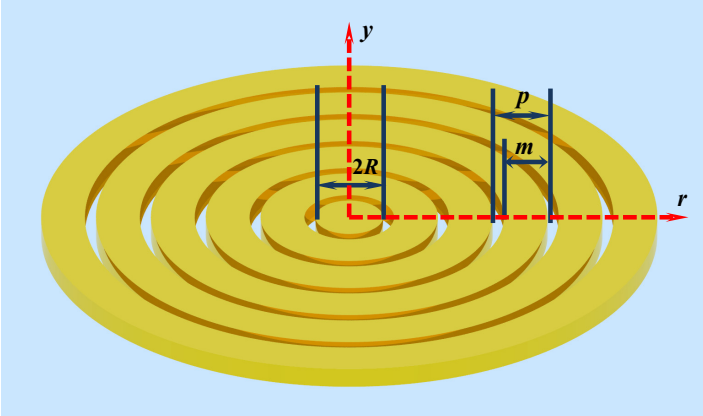

Fig. 1. Illustration of a disc resonator with a ring grating in a homogenous dielectric environment. The geometrical parameters are defined in the figure. Quantities are given in the text.

Figure 1 shows the schematic of the investigated structure. The central component is a gold nanodisc with radius $R = 90$ nm. Concentric rings are placed around the nanodisc. The radial grating is characterized by a period p and a filling factor m/p, with m being the thickness of the metallic rings. The corrugation is assumed to be perfect, i.e. sections of the grating consist of either metal or dielectric material. All components share the same height of $h = 30$ nm. The structure is embedded in a homogeneous dielectric ($\varepsilon_{\text{glass}} = 2.07$) and illuminated by a linearly polarized plane wave propagating in the y direction. In such a configuration, only antisymmetric SPPs mode [30] can be excited in the metal films [31]. The normal electric field components of the SPPs above and below the metal layer are out-of-phase.

Similar to a nanowire resonator, made from a thin elongated metallic wire, the resonance condition of disc resonators can be derived in analogy to ordinary Fabry-Perot resonators. The only difference concerns the spatial distribution of the modes that is described by a Bessel function instead of sinusoidal functions. To observe a resonance in a circular disc requires the total phase, including the phase accumulated upon propagation across the disc $2k_{\text{spp}}R$ and a contribution from the complex reflection coefficient ϕ at the terminations [32,33], to amount to $2k_{\text{spp}}R + \phi = 2N(J = 0)$. Here, $N(J = 0)$ refers to the n^{th} root of the Bessel function of the first kind and k_{spp} is the propagation constant of the SPPs mode at the frequency of interest.

Theoretically, the concentric rings should be positioned according to the roots of Bessel

#236122 - $15.00 USD Received 12 Mar 2015; revised 16 May 2015; accepted 18 May 2015; published 26 May 2015

functions. However, as explained above, a pure mathematical Bessel function is not appropriate to predict the ring positions. Even though the rings are placed at the positions calculated by the model of the Bessel mode resonator, the corrugations of the actual structure introduce further complex phase perturbations as the SPPs propagate towards the central antenna. Without taking these additional phase complexities into account, the rings placed at the predicted positions are unable to provide the optimal result. In general, the ideal parameters of the concentric rings can only be obtained by elaborate optimizations on each ring. This is extremely time consuming and impractical for a truly three-dimensional geometry. On the contrary, we can take advantage of the geometrical symmetry, i.e. a cylindrical structure can be assumed as the rotation of a two-dimensional geometry. The performance of such ring grating is governed by only a few parameters, which greatly simplifies the optimization process. Therefore, we opt to choose a regular radial periodic grating as the supporting structure around the central disc antenna. Nevertheless, for the completeness of the study on the circular ring gratings, we compare the performance of the periodic grating rings to the other similar structured rings at the end of this section. Specifically, we consider a Bessel ring grating obtained by fitting the radial distance of each ring to the roots of the Bessel function and an elaborate optimized grating ring structure. The optimization process associated with the latter ring structure is only technically possible for a small number of rings. Eventually we show that the fully optimized structure only attains a marginal improvement, justifying the use of periodic grating rings.

When the structure is illuminated, the circular grating acts as a plasmon coupler comparable to its one-dimensional counterpart, i.e. the curved slits convert the incident light into SPPs by providing extra momentum. Because of normal incidence inward and outward propagating SPPs are equally excited. In such concentric rings, the energy of the inward propagating SPPs is converging as it is guided towards the central disc antenna, whereas the diverging outward propagating SPPs will not contribute to the field enhancement in the central antenna. Therefore, only the inward propagating SPPs are of relevance in this paper. The discussions on the grating functionalities are also based on the SPPs propagating toward the central disc antenna.

For the inward propagating SPPs, carefully tailored gratings manipulate the phase accumulated upon propagation. At resonance, the SPPs launched by each ring interfere constructively in the central disc antenna. This requires a 2π phase difference in each ring. Simultaneously, 2π phase accumulation in one grating period also fulfills the Bragg reflection condition, i.e. $k_{\mathrm{spp}}p = n\pi$, where $n = 2$ holds in this situation. This suggests that the circular grating will prevent the outcoupling of SPPs bouncing back and forth in the central disc. When Bragg reflection occurs at the frequency where the central disc resonator shows its intrinsic resonance, the amplitude of the reflection coefficient is maximized, i.e. the structure is optimized.

Using a similar procedure as already being applied to one-dimensional gratings [34], we optimized the free parameters of the ring grating to maximize the field enhancement in the central disc antenna. This has been done by calculating the optical response of the system using the open source finite-difference time-domain (FDTD) software Meep [35,36]. The FDTD method is a fully explicit numerical technique widely used to model photonic systems. In FDTD, electromagnetic fields are discretized on a Yee grid and Maxwell's equations are solved in time domain with a leap-frog algorithm. For the dispersive materials such as gold used in this paper, the material dispersion is implemented as a sum of harmonic resonance.

Here we have to emphasize that although the geometrical symmetry can be used to simplify the optimization process, all the numerical results presented in this work are calculated in three dimension since the entire configuration including the illumination source does not possess the cylindrical symmetry. Therefore, the numerical simulations are quite time consuming. For instance, to obtain one spectrum with five optimized grating rings needs approximately one week time even with 128 CPUs. Nevertheless, FDTD is the most suitable method for the investiga-

#236122 - $15.00 USD Received 12 Mar 2015; revised 16 May 2015; accepted 18 May 2015; published 26 May 2015

tions in this work. Comparing to the other methods, e.g. Fourier Modal Analysis, FDTD can cope well with large structures. Circular geometries can also be treated perfectly with appropriate spatial discretization. For all the simulations presented in this paper, spatial discretization was chosen to be 5 nm. Furthermore, since the calculations are performed in the time domain, all quantities of interest can be directly accessed and the numerical results are intuitive for physical interpretation.

In the simulation, the intensity of the normal electric field component 20 nm above the metal surface is recorded and taken as a measure to characterize the resonance of the nanoantenna. This field component is not contained in the illumination. It is, therefore, a quantity that is purely characteristics for the excitation of the localized eigenmode. The enhancement factors for the other field components show the same dependency since the ratio between the different field amplitudes is locked by the modal properties. Moreover, given that the same SPP mode is excited in the bare nanodisc and in the nanodisc surrounded by the optimized grating rings, the field amplitude decays at the same rate in both cases (with and without rings) as the recording plane moves away from the metal surface. This suggests that the improvement of the structure with grating rings does not depend on the recording plane. Therefore, this single field component is sufficient to analyze the resonance property of the nano antenna.

In the optimization process, a first educated guess for the grating period can be made by comparing it to the wavelength of the excited SPP at the resonance frequency of the nanodisc. In general, gratings with higher filling factor of metal are preferred. The large metal content within a period substantially diminishes the scattering loss as the SPP mode propagates on the corrugated structure, i.e. wider channels lead to a cut-off of SPP mode because of the interaction with the channel modes inside the grooves. Therefore, in the remaining part of this paper, the filling factor of the ring gratings is set to be 90%.

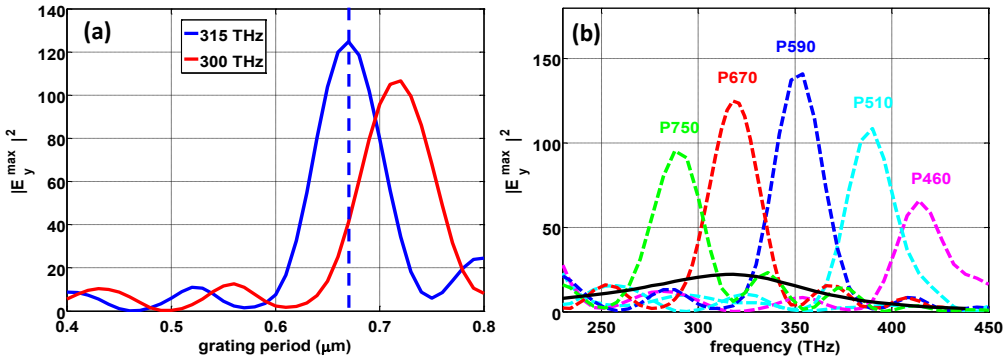

Fig. 2. (a) Maximum intensity of the normal electric field component $|E_y^{max}|^2$ recorded 20 nm above the surface of the central nanodisc when the periodicity of the surrounded ring gratings varies. The blue curve is obtained by illuminating the structure with a plane wave at the resonance frequency of the bare disc (315 THz). The optimal grating period (indicated by the blue dashed line) approximately equals the SPP wavelength. The red curve is obtained with an off-resonance illumination frequency of 300 THz. (b) Spectral characteristics of the nanodisc endowed with circular gratings of different periodicity (dashed lines) and without grating (black solid curve). The spectrum with optimized grating period (670 nm) is plotted by the red dashed line.

Theoretically, a larger ring number is preferred since more impinging illumination light can be harvested. In practice, the actual field enhancement is limited by the propagation length of the SPPs. In the present configuration the guided SPP has a propagation length of approximately

#236122 - $15.00 USD Received 12 Mar 2015; revised 16 May 2015; accepted 18 May 2015; published 26 May 2015

5μm. This suggests in the lowest order approximation that five rings are sufficient to constitute a SPPs reflector. In fact, SPPs are still reflected by the additional rings but they cannot return to the nanodisc due to dissipation. Nevertheless, the resonance in the central nanodisc can be further enhanced by these additional rings serving as conventional SPPs couplers although their contributions drop rapidly. Particularly, the central nanodisc benefits mainly from closely surrounding rings. For this reason, we consider a circular grating made of five rings in this part of the work.

Figure 2(a) displays the maximum field intensity 20 nm above the nanodisc surface when it is endowed by circular gratings with varying periodicity. The illumination frequency associated with the blue curve is chosen to be the resonance frequency of the bare nanodisc (315 THz). To enhance the resonance of the central disc while preserving its resonance frequency, the surrounding ring grating is required to be resonant at the same frequency. Thus, $k_{\mathrm{spp}}L = 2n\pi$ has to hold, which is equivalent to $L = n\lambda_{\mathrm{spp}}$, where λ_{spp} is the wavelength of the guided SPP and n is an integer. L is the radial length of the surrounding grating, i.e. $L = np$, with $n = 5$ in the considered structure. Therefore, the optimal grating period can be predicted, i.e. $p \approx \lambda_{\mathrm{spp}}$ when the phase discontinuity at each grating gap is neglected because of the large filling factor (90%). This prediction is consistent with the results shown in Fig. 2(a). Circular gratings whose periodicity approximately equals the wavelength of the guided SPP can significantly enhance the field intensity in the central nanodisc. Similar to an aperture surrounded by circular periodic corrugations [22], that the aperture transmission exhibits a peak when the launched SPP wavelength coincides with corrugation periodicity, the field intensity of the enclosed disc resonator considered here is also remarkably strengthened under the same condition. For illustration purposes, an additional curve with an off-resonance illumination frequency (red curve, 300 THz) is presented in Fig. 2(a) as well. The spectral misalignment between the Bragg resonance and the disc resonance causes the field enhancement to be inferior.

In Fig. 2(b), we compare the spectral characteristics of nanodiscs endowed with ring gratings of different periodicity. The resonance spectrum of a bare nanodisc is plotted as a reference (black solid curve). The spectra obtained with gratings of different periodicity exhibit a contour similar to the resonance spectrum of the bare nanodisc. Apparently, the resonance of the bare nanodisc gets enhanced by the circular gratings. However, the absolute value of the field enhancement depends sensitively on the chosen period. The previously identified optimized period for the ring grating (670 nm), where the Bragg resonance matches the resonance of the nanodisc, does not exactly provide the highest field intensity. A slightly detuned period performs better in that sense as shown by the numerical results.

Moreover, it can be seen that ring gratings with strongly mismatched periods do not contribute to the field enhancement in the nanodisc antenna. Destructive interference of the excited SPPs will suppress the field intensity. In the extreme case, the field intensity in the nanodisc almost vanishes at the resonance frequency of 315 THz when the grating period equals to 460 nm. Even though the central nanodisc is perfectly excited, it is visually concealed by the surrounding rings.

The line width of the emerging resonance is closely related to the line width of the Bragg resonance. For a specific grating period, only the SPPs modes of the designed frequency can propagate through the periodic corrugations and are eventually guided into the central resonator. SPPs modes of different frequencies will be suppressed by destructive interference before they reach the central resonator. From this perspective, the structured metallic film shapes the spectrum of the illumination on the central disc resonator, modifying the spectral characteristics of the resonance.

As mentioned previously, the maximum number of rings which contribute to resonance enhancement is ultimately restrained by the propagation length of the respective SPPs mode. On

#236122 - $15.00 USD Received 12 Mar 2015; revised 16 May 2015; accepted 18 May 2015; published 26 May 2015

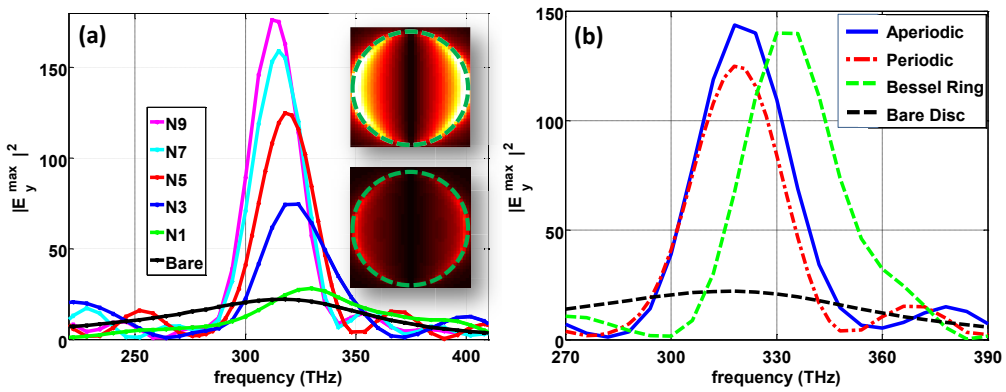

Fig. 3. (a) Spectral characteristics of the nanodisc antenna endowed with circular gratings of different ring numbers. The insets display the amplitude of the normal electric field component above the nanodisc with five optimized rings (upper) and without rings (lower). Both are resonant fields recorded at the resonance frequency of 315 THz. The insets share the same color scale. (b) Spectral characteristics of the nanoantenna endowed with a periodic ring grating (periodicity 670 nm and five periods are considered, red dash-dot line), five rings whose radial distances are fitted to the roots of Bessel function (green dashed line), and five aperiodic optimized rings (blue solid line). All the evaluated structures are embedded in the symmetric dielectric environment. Black dashed line depicts the dispersive characteristic of the bare nanodisc for comparison.

the contrary, with an insufficient number of rings the circular grating is not properly functional either. To probe for a reasonable number of rings, Fig. 3(a) compares the maximum field intensity of the nanodisc antenna supported by different numbers of rings. Here, all the ring gratings have the optimized periodicity of 670 nm and 90% filling factor.

Apparently, one ring is not adequate to constitute a circular grating. This single metallic ring hardly assists the nanodisc to achieve any enhancement for the field intensity. The Fano-like asymmetric spectral response (green solid line) implies a notable coupling between the nanodisc and the single ring. As the number of rings increases, the concentric rings transform into a circular grating and boost the field intensity in the central disc antenna. For the considered SPPs mode, five to seven rings are fully sufficient to achieve the desired enhancement for the field intensity in the central nanodisc. The reflectivity is already saturated with five grating rings, the further increase of field intensity is attributed to the improved SPPs excitation by additional rings. However, limited by the propagation length of the SPPs mode, the increment becomes less pronounced and quickly converges, as shown in the Fig. 3(a). Therefore, it is not necessary to consider circular gratings with more than five rings.

From Fig. 3(a) we can evaluate the quality factor of the central disc resonator. With five optimized periodic grating rings, the quality factor reaches 11, much higher than that of the bare nano disc ($Q = 2.86$). It worth noticing that even though the field intensity can be further enhanced by attaching more surrounding rings, the quality factor has no significant increment, e.g. $Q = 12$ with nine rings. In the view of quality factor enhancement, additional rings hardly provide further improvement.

More importantly, as we can see from the insets in Fig. 3(a) where the amplitudes of the normal electric field component above the central disc are shown, the supporting ring structure does not perturb the mode profile of the nanoantenna. In both cases, the disc with and without the supporting grating, the typical two lobes of the specific electric field component can be seen. The field profile corresponds to that of a Bessel function of the first kind around the central

#236122 - $15.00 USD Received 12 Mar 2015; revised 16 May 2015; accepted 18 May 2015; published 26 May 2015

coordinate. This indicates the excitation of the fundamental dipolar mode. The only notable difference is the enhanced field amplitude for the disc with the optimized circular grating. Here, both field amplitudes are plotted with the same color scale.

According to the aforementioned reasoning in the beginning of this section, directly matching the rings positions to the roots of the Bessel function is not optimal for the supporting rings. In general, in such a cylindrically symmetric geometry, rings arranged in a pattern according to the Bessel function profiles are always assumed to be the optimal design at the first glance. However, under certain circumstance, the optimal design is not predicted by the Bessel functions, e.g. in the situation considered here. To illustrate this aspect, Fig. 3(b) compares the spectral characteristics of the central nanodisc endowed by three different supporting ring structures. The Bessel ring structure consists of fives rings whose radial distances are set to coincide the even ordered roots of the Bessel function of the first kind. Clearly illustrated in Fig. 3(b), Bessel rings can achieve a slightly higher enhancement (green dashed line) but at the obviously shifted frequency when compared to resonance peak with five periodic rings (red dot-dash line). The design purpose of this ring disc nanoantenna is to enhance the resonant strength of central antenna without tuning its resonance frequency. Apparently, with inferior enhancement at the designed frequency of 315 THz, this Bessel ring grating is not optimal.

In fact, to simultaneously obtain resonance enhancement and to preserve the resonance frequency requires individual optimizations on the position of each ring. This is a computationally demanding task, therefore a ring structure containing only five rings is evaluated. The optimization process is performed in a sequential manner. We start with the simplest configuration, i.e. one ring around the central disc. The optimal position of the first ring is identified when both criteria are simultaneously fulfilled. This is attained by sweeping the parameter spaces. Then, the second ring is introduced into the hybrid structure. The optimization process of the second ring is performed while maintaining the optimized result of the first ring. Continuing with the same procedure, five optimized ring positions are determined. The radial distances from disc center to the outer edge of each ring are 790 nm, 1420 nm, 2040 nm, 2720 nm and 3360 nm. These rings constitute an aperiodic grating. Specifically, the radial distances between two adjacent rings are 700 nm, 630 nm, 620 nm, 680 nm and 640 nm. Obviously, this does not coincide with the roots of Bessel function.

From Fig. 3(b), even though each ring is precisely located, the aperiodic rings only achieve an incremental improvement when compared to the periodic structure. In principal, the aperiodic rings do not change the fundamentals of the physical aspects. Since each ring has to be optimized individually, it takes much longer time to identify the optimal design. In contrast, the optimization of a periodic grating structure is much more convenient, reliable, and fast since the geometry is characterized by only a few free parameters. Moreover, since the periodic structure is more reliable in terms of fabrication feasibility and the optimization process can be largely simplified, in the next section we extend the investigations on the metallic ring disc structure embedded in the asymmetric dielectric environment with the periodic structure.

3. Analysis for an asymmetric dielectric environment

In the previous section, we have demonstrated that the resonant field intensity of the central disc antenna will be strongly enhanced when it is surrounded by an optimized circular grating. However, to make use of the enhanced near field, at least one surface requires to be experimentally accessible. Thus, we consider in the following an asymmetric dielectric environment, i.e. the grating endowed disc antenna is situated on a glass substrate. The cladding is assumed to be air. The illumination remains a linearly polarized plane wave and is normally incident from the substrate. This choice is motivated by the experiments described below.

Figure 4(a) illustrates the spectrally dispersive characteristics of a disc antenna endowed with

#236122 - $15.00 USD Received 12 Mar 2015; revised 16 May 2015; accepted 18 May 2015; published 26 May 2015

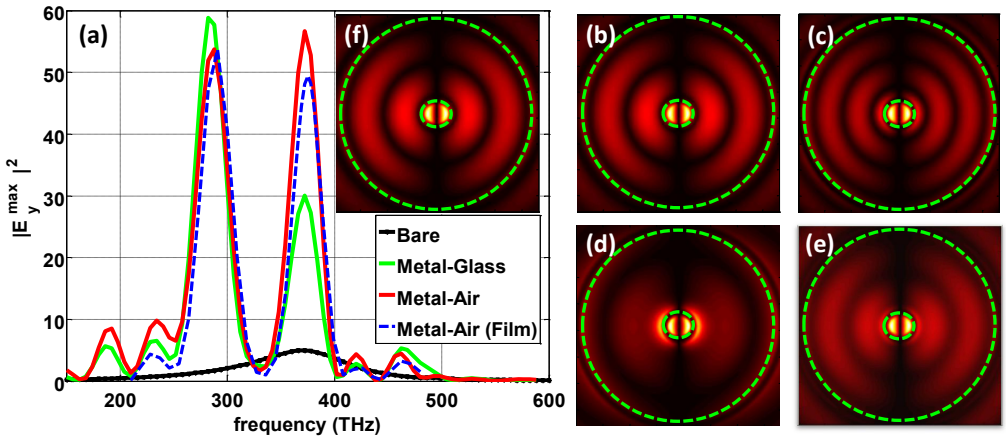

Fig. 4. (a) Spectral characteristics of a disc resonator endowed with five optimized rings in an asymmetric dielectric environment. The optimized grating parameters are obtained by taking the maximum field intensity of the normal electric field component $|E_y^{\max}|^2$ 20 nm above the metal-air interface of the central nanodisc (red solid curve) as the optimization criterion. The black curve corresponds to the spectral characteristic of an isolated disc resonator in the asymmetric dielectric environment. For the sake of completeness, the maximum field intensities 20 nm below the metal-glass interface are also presented (green solid curve). Blue dashed curve depicts the same quantity as the red solid curve but with additional metal film around the entire ring disc structure. This is consistent with the actual experimental configuration. (b) and (c) Normal electric field amplitude $|E_y|$ 20 nm above the metal-air interface and below the metal-glass interface at the resonance peak of 375 THz. (d) and (e) Normal electric field amplitude $|E_y|$ 20 nm above the metal-air interface and below the metal-glass interface at the resonance peak of 288 THz. (f) Same field quantity as (b) but with closed metal film around the entire ring disc structure. Only the central fields covering the disc and the first ring are shown in (b)–(f) such that the field profiles are readable. The disc and the outer edge of the first ring are marked in each figure by green dashed line. Color scales for all the figures are the same.

five optimized periodic rings in the asymmetric dielectric environment. Because only the field enhancement at the metal-air interface can be exploited, the intensity maxima of the normal electric field 20 nm above the metal-air interface of the nanodisc are extracted as a function of the illumination frequency and used to show the resonance spectrum (red curve) in Fig. 4(a).

Unlike the resonance spectrum obtained in a symmetric dielectric environment, two peaks appear in Fig. 4(a). They correspond to the excitation of two degenerated frequency-shifted resonant film modes (quasi-symmetric and quasi-antisymmetric) in the asymmetric dielectric environment. The optimized grating periodicity is retrieved from the maximum field intensity 20 nm above the metal-air interface at the resonance frequency of the bare nano disc (375 THz), corresponding to the excitation of the quasi-antisymmetric film mode. Here, based on the same optimization procedure as for the symmetric dielectric environment, we identify the optimized grating period to be 810 nm. All the other parameters remain unchanged, i.e. five rings with 90 % filling factor.

From Fig. 4(a) it can be seen that, compared to the isolated disc resonator (black curve), the field intensity of the nanodisc endowed with a circular grating is significantly enhanced and the line width of the resonance peak is largely reduced. Accordingly, the other resonance peak, occurring at 288 THz, corresponds to the quasi-symmetric film mode. To better visualize the properties of these two modes, normal electric field amplitudes recorded 20 nm above and

#236122 - $15.00 USD Received 12 Mar 2015; revised 16 May 2015; accepted 18 May 2015; published 26 May 2015

below the metal film at two resonant frequencies are given in Fig. 4(b)–4(e). To ensure the readability of the image, only the central range of the field covering the central disc and the first ring are shown.

We calculated the quality factor for the central disc antenna at the resonance frequency of 375 THz. With only five optimized grating rings, the quality factor amounts to almost $Q = 17$, much higher than that without circular grating ($Q = 3.5$). This substantial increase of the quality factor can be attributed to the functionality of the supporting ring grating.

In the actual experiment setup, the ring disc structure is surrounded by a metal film, which is deposed on the glass substrate. This metal film is not removed with the purpose to increase the signal-to-noise ratio in the SNOM measurement. Nevertheless, the spectral response of the central disc antenna is not disturbed by the additional metals [blue dashed curve in Fig. 4(a)] except the slightly smaller magnitude of the second resonance peak when compared to the situation without the metal film [red solid curve in Fig. 4(a)]. This can be explained by the inefficient excitation since the incident light is blocked by the closed metal film. In fact, the metal film has no influence on the field distributions of central disc resonator, as indicated by the identical fields shown in Fig. 4(b) (without metal film) and Fig. 4(f) (with metal film).

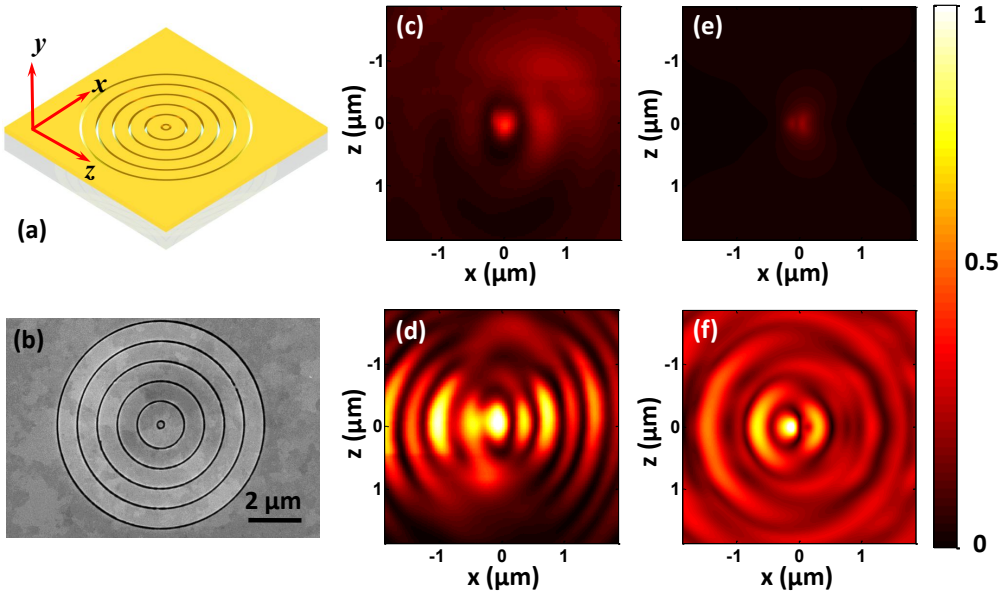

Fig. 5. (a) Sketch of the nanodisc endowed with a circular grating in an asymmetric dielectric environment in the experiment. (b) SEM image of the fabricated sample. (c) and (d) SNOM measurements of the near field distribution in a bare and a circular grating endowed nanodisc. (e) and (f) Simulated near fields in a bare and circular grating endowed nanodisc.

To substantiate the simulations by experiments, we fabricated two samples. The reference sample was just a single gold disc on a fused silica substrate. The second sample consisted of a disc of the same size surrounded by five concentric rings of optimized parameters (810 nm period with 90 % filling factor). Focused ion beam milling of an evaporated gold film was used to fabricate both samples. We probed the spatial distribution of the fields at the resonance frequency with a scanning near field optical microscope.

In agreement with FDTD simulation, the structure was illuminated through the glass substrate with a linearly polarized broad Gaussian beam at a frequency of 382 THz (wavelength 785 nm). The SNOM was equipped with a tapered fiber tip coated with gold, leaving a 180

#236122 - $15.00 USD Received 12 Mar 2015; revised 16 May 2015; accepted 18 May 2015; published 26 May 2015

nm aperture at the apex and operated in the collection mode. As mentioned above, to increase the signal-to-noise ratio, the hybrid structure was cut out from a metal film in the experimental configuration, as shown in Fig. 5(a). The SEM image of the fabricated sample is shown in Fig. 5(b). With the surrounding metal film, the transmitted scattering light was blocked for the experiment while the optical process considered in this paper will not be influenced. Moreover, the thickness of metal layer was increased to 50 nm in the experiments to further suppress the transmission.

Figure 5(c)–5(f) compare the SNOM measurements of the near field distribution in a bare nanodisc [Fig. 5(c)] and a nanodisc endowed by a grating with five optimized rings [Fig. 5(d)] to the respective simulations [Fig. 5(e) and 5(f)]. All experimental modifications used in our previous considerations were taken into account when performing the simulations as shown in Fig. 5(e) and 5(f). In the SNOM measurement, only the transverse fields are collected, i.e. the field components perpendicular to the tip axis are measured. In reality, the SNOM tip is approximately 30° tilted with respect to the surface normal within the yz-plane rather than perfectly vertical to the metal surface. The normal electric field component is partially recorded in the experiment and contributes to the measured signal. This phenomenon has been taken into consideration in the simulations by including the projections of the relevant field components. Moreover, the observed field distribution in the experiment is influenced by the SNOM resolution. This is constrained by the diameter of SNOM aperture which is approximately 180 nm. With this resolution, it is impossible to resolve the finer field distributions above the nanodisc. Considering the tilt and the metal coating, the center of the aperture was actually further away from the surface. Therefore, the recording plane in the simulation is moved $\sim$100 nm away from the metal surface. The experimental results show good agreement with the theoretical calculation, thereby confirming the working principle for enhancing the antenna resonance.

Both in experiment and simulation, the illumination is linearly polarized in x direction. The dipolar resonance supported by the nanodisc is naturally aligned into the same direction. This feature can be clearly identified in the field distributions of Fig. 5. In addition, the SPPs' interference fringes above the grating rings can be recognized both in the experimental images and in the FDTD simulations. As the result of a coherent superposition of the excited SPPs, the field amplitudes appear stronger close to the central disc antenna. This proves that circular gratings convert the incident light into SPPs and effectively focus the energy into the central resonator.

Moreover, experiments [Fig. 5(c) and 5(d)] and simulations [Figs. 5(e) and 5(f)] are respectively shown on the same color scale, making the strength of the fields comparable between the different samples. Most notably, we observe a remarkable enhancement of the field amplitude above the disc antenna when it is endowed with the optimized grating. Overall, this proves the applicability of the concept and demonstrates that the supporting circular structure can be employed to enhance the resonance of the disc antenna, allowing further specific plasmonic applications.

4. Conclusion

We have numerically verified that a few concentric rings suffice to constitute a circular grating that collects incident illumination from an extended area and confines the launched energy into the central resonator. The strengthened near field above the central nano resonator is substantiated by the experiments. The key requirement is to choose the grating parameters in such a way that the phase difference of the guided SPPs in radial direction induces a constructive interference in the central resonator. This leads to a significantly enhanced field intensity in the enclosed resonator and therefore increases the quality factor by at least half an order of magnitude. The associated high field intensity and spectral sensitivity are beneficial for sensing devices, nonlinear photonic elements and in cavity quantum electrodynamics experiments.

#236122 - $15.00 USD Received 12 Mar 2015; revised 16 May 2015; accepted 18 May 2015; published 26 May 2015

Acknowledgments

Support by the German Federal Ministry of Education and Research (PhoNa), by the Thuringian State Government (MeMa), and the German Science Foundation (SPP 1391 Ultrafast Nano-optics) is acknowledged. We acknowledge support by Deutsche Forschungsgemeinschaft and Open Access Publishing Fund of Karlsruhe Institute of Technology.

#236122 - $15.00 USD Received 12 Mar 2015; revised 16 May 2015; accepted 18 May 2015; published 26 May 2015